Table 2 Normalized airfoil drag coefficients

	C_d/C_{d0}^a		
Re_c	$\alpha = 0$ deg	$\alpha = 5$ deg	$\alpha = 10$ deg
57×10^3	0.6155	0.8534	0.9389
100×10^3	0.7054	0.3870	0.2475
150×10^3	——	——	0.7596

[a]Drag coefficient without excitation/drag coefficient with excitation.

that acoustic excitation significantly narrows the wake at all three angles of attack. Notice that once the separation on both sides of the airfoil has been suppressed at $\alpha = 0$ deg (Fig. 1a), the mean profile is symmetric as expected. In addition, the wake shifts down, following the incline of the trailing edge at $\alpha = 5$ and $\alpha = 10$ deg (Figs. 1b and 1c), similar to airfoil wakes at high Reynolds numbers when the Kutta condition is satisfied.

A quantitative analysis of the effect of acoustic excitation on airfoil performance is based on the drag coefficient results (Table 2), obtained by integration of the mean-wake profiles. The most significant reduction of the drag coefficient is achieved for $Re_c = 100 \times 10^3$, with the drag coefficient reduced by 75% at $\alpha = 10$ deg. It is also obvious that a greater decrease of the drag coefficient is achieved for $Re_c = 100 \times 10^3$ than for $Re_c = 57 \times 10^3$, except for $Re_c = 57 \times 10^3$ at $\alpha = 0$ deg. Indeed, separation regions, comparable in size for these two Reynolds numbers at corresponding angles of attack, were only reduced for $Re_c = 57 \times 10^3$, whereas they were suppressed for $Re_c = 100 \times 10^3$ with the same power input. It can be concluded that higher amplitude excitations are needed to influence the airfoil performance at lower Reynolds numbers. Note that decrease of the drag coefficient for $Re_c = 100 \times 10^3$ becomes more pronounced as the angle of attack increases (Table 2). This trend is due to suppression of the separation region, which increases as angle of attack increases. The improvement of the airfoil performance for $Re_c = 150 \times 10^3$ is less significant than it is for the $Re_c = 100 \times 10^3$. Nevertheless, a separation region on the upper surface of the airfoil was suppressed by acoustic excitation, and a 24% decrease of the drag coefficient resulted.

To assess the effect of acoustic excitation on coherent structures in the airfoil wake, transverse velocity component spectra E_{vv} are presented. Figure 2 shows the E_{vv} spectra for $Re_c = 100 \times 10^3$ at $x/c = 3$. The peaks in the spectra associated with the unexcited flow are clear evidence of vortex shedding in the airfoil wake at all angles of attack. Peaks corresponding to 0-, 5-, and 10-deg angles of attack centred at 20, 20, and 14 Hz are strongly attenuated, broadened and shifted to 30, 40, and 40 Hz, respectively, suggesting that vortex coherency and length scale are decreased by acoustic excitation. It can also be inferred from comparison of the results in Fig. 2 and Table 1 that the optimum excitation frequency does not match the vortex-shedding frequency but is an order of magnitude greater. It is speculated that the optimum frequencies found in this investigation match the separated shear layer instability frequencies, agreeing with the results of Refs. 2 and 4. Note that the effect of the acoustic excitation on the vortex shedding for this Reynolds number is similar to the effect on the drag coefficient (Table 2) because a more significant diminishment of the peaks in the spectra is achieved for higher angles of attack.

Conclusions

External acoustic excitation at particular frequencies and suitable amplitudes can substantially reduce or suppress the separation region of an airfoil so that an increase in lift and/or a decrease in drag result. The effect of the excitation strongly depends on the excitation frequency and amplitude. In particular, the effective-frequency range decreases with a decrease of the excitation amplitude. For a constant amplitude excitation, this range narrows with a decrease of the Reynolds number or increase of the angle of attack. It is speculated that the optimum frequencies found in this investigation match separated shear-layer instability frequencies, in agreement with Refs. 2 and 4. The results also suggest that higher amplitude excitations are needed to influence the airfoil performance at lower Reynolds numbers.

The acoustic excitation alters wake structure, decreasing the vortex length scale and the coherency of the vortices. Also, the magnitude of the acoustic excitation effect on the wake structure correlates with the extent of the improvement in the airfoil performance.

Acknowledgments

This research was supported by the Natural Science and Engineering Research Council of Canada through operating and equipment grants. The authors thank Jerry Karpynczyk for his help with the experimental setup.

References

[1]Lissaman, P. B. S., "Low Reynolds Number Airfoils," *Annual Review of Fluid Mechanics*, Vol. 15, 1983, pp. 223–239.

[2]Hsiao, F. B., Jih, J. J., and Shyu, R. N., "The Effect of Acoustics on Flow Passing a High-AOA Airfoil," *Journal of Sound and Vibration*, Vol. 199, No. 2, 1997, pp. 177–178.

[3]Zaman, K. B. M. Q., "Effect of Acoustic Excitation on Stalled Flows over an Airfoil," *AIAA Journal*, Vol. 30, No. 6, 1992, pp. 1492–1499.

[4]Zaman, K. B. M. Q., and McKinzie, D. J., "Control of Laminar Separation over Airfoils by Acoustic Excitation," *AIAA Journal*, Vol. 29, No. 7, 1991, pp. 1075–1083.

[5]Mallon, K. J., Levinski, O. P., and Brown, K. C., "Experimental Investigation of the Unsteady Aerodynamics of a Symmetric Aerofoil at Low Reynolds Numbers," *Proceedings of Second Pacific International Conference on Aerospace Science and Technology/Sixth Australian Aeronautical Conference*, Vol. 1, Institution of Engineers Australia/Royal Aeronautical Society, Melbourne, Victoria, Australia, 1995, pp. 475–484.

A. Plotkin
Associate Editor

Robust-Optimal Design of a Lightweight Space Structure Using a Genetic Algorithm

D. K. Anthony* and A. J. Keane†
University of Southampton, Southampton, England SO17 1BJ, United Kingdom

I. Introduction

WHEN using a "perfect" computer model of a structure to optimize its dynamic (vibration) performance, the results rely on the exactness of the model and can in practice be very sensitive to small changes in design variables. This is especially the case in the mid- and high-frequency regions where modal overlap occurs. To assess this, the multidimensional gradient of the search space at the current design point can be approximated, or changes in the performance of the structure caused by "local" variations in design variables can be calculated. Both of these normally carry a high computational expense, especially for high-dimensional problems.

Here the optimization of a structure using genetic algorithms (GA)[1] is described, for which the robustness of the structure's performance is also considered. One type of GA used efficient methods

Received 29 July 2002; revision received 1 February 2003; accepted for publication 21 March 2003.

*Research Fellow, Department of Mathematics, Highfield; currently Research Fellow, Instituto de Acústica (CSIC), C/Serrano 144, Madrid 28006, Spain.

†Professor, Computational Engineering and Design Center, School of Engineering Sciences, Highfield.

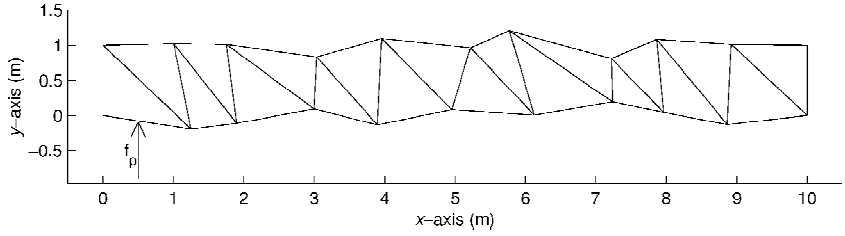

Fig. 1 Best optimization structure geometry using nominal performance only to minimize vibration transmission along the structure.

to estimate local variations about the current design point, and another was a previously reported noisy phenotype GA in what appears to be its first reported application to a dimensionally large problem. Comparisons are made of the effectiveness and efficiency of these methods.

II. Optimization Problem

The authors previously reported the optimization of the dynamic performance of a 40-beam two-dimensional lightweight cantilever truss space structure to minimize the vibration transmission from the base to the end of the structure.[2] The structure consisted of 10 square bays, each with a diagonal element. The Euler–Bernoulli beams had identical properties: axial rigidity = 69.80 MN, bending rigidity = 12.86 kNm^2, and mass per unit length = 2.74 kg/m. The structural damping of each of the normal uncoupled beams modes was fixed to have a bandwidth of 20 s^{-1}. A GA was used to minimize the vibrational energy transmission by optimizing the x and y coordinates of the 18 middle joints, represented by vector $\boldsymbol{x}$. A fitness function representing the average vibrational energy level in the right-most beam between 175 and 195 Hz, $f(\boldsymbol{x})$, was used. This was calculated using a modal dynamic receptance analysis, as described in the reference. The best structure geometry found is shown in Fig. 1, which achieved a reduction of 47.5 dB in $f(\boldsymbol{x})$.

The sensitivity of the evaluation of $f(\boldsymbol{x})$ was studied by adding sets of geometric perturbations and reevaluating the average vibrational energy level. Some structures were more robust than others, and a structure that is nominally superior is not always the best in practice. The average deterioration of the mean performance was found to be by 5.2 dB (5.0 dB for the structure shown in Fig. 1), although for one structure this figure was as high as 10.5 dB. This analysis is discussed in the following section. The idea behind the work described here is to use the perturbed (geometry) performance of the structure during the GA instead of a postoptimization sensitivity analysis, so as to produce optimal and robust design solutions.

III. Robust Optimization Methods

Both the strategies considered require reevaluations of the average energy level with slightly altered geometries (except in one case) and thus increase the computational effort required by a factor, denoted by N.

A. Computer Experiment Methods

The sensitivity of any intermediate or final design solution in the face of small geometric perturbations can be studied by adding a set of N perturbation vectors ($\Delta\boldsymbol{x}_i$) to $\boldsymbol{x}$ to generate a perturbed objective function vector $\boldsymbol{f}^p$ of length N (Ref. 2). For a structure design $\boldsymbol{x}_j$

$$\boldsymbol{f}_j^p(i) = f(\boldsymbol{x}_j + \Delta\boldsymbol{x}_i), \qquad i = 1, N \tag{1}$$

A 95% probability limit f_{95} can be used to estimate the performance [the largest value of $f(\boldsymbol{x})$ in this case] that is only expected to be exceeded for 5% of perturbations. f_{95} is defined as

$$\text{num}\left[\boldsymbol{f}_j^p < f_{95}(\boldsymbol{x}_j)\right] = 0.95N \tag{2}$$

where num[ ] defines the number of elements of $\boldsymbol{f}_j^p$ satisfying the condition. Previously the authors used this measure to evaluate the robustness of the final designs resulting from the GA.[2] $\Delta\boldsymbol{x}_i$ was uniformly distributed over range $\pm v$, where $v = 0.01$ m in this instance. An accurate estimate of f_{95} was achieved with $N = 300$ (denoted $f_{95:300}$). The precise value of v was found not to be important if the magnitude were small and within the "linear" range of the structure's geometrically perturbed performance.[2] It is not practical to use $f_{95:300}$ as the fitness function during optimization as this would increase the computational effort required by a factor of $N(=300)$. More efficient estimates of f_{95} were used.

1. *One-at-a-Time Experiments ($\hat{f}_{95:OAT}$)*

So-called one-at-a-time (OAT) experiments are extensively used in engineering. Here $N = 37$, and the $\Delta\boldsymbol{x}_i$ are a null vector and 36 vectors with each element individually set to a value of $+v$. The main disadvantage of this approach is that factor interactions are ignored. If significant interactions exist this strategy will usually produce inaccurate results.

2. *Taguchi Orthogonal Arrays ($\hat{f}_{95:64}$ and $\hat{f}_{95:L81}$)*

A better strategy than the OAT method would be to conduct a full-factorial experiment, in which the response to all of the combinations of factor levels is determined. For more than a small number of factors, the number of experiments required is large. Fractional factorial design requires significantly less experiments and assumes that higher-order interactions are insignificant. Here two of Taguchi's designs[3] are used: 1) the L64 array, a 64-experiment design for 63 two-level factors [$N = 64$ and $\Delta\boldsymbol{x}_i$ is defined by the array rows, where the factor values (1, 2) are mapped onto $(0, +v)$]; 2) the L81 array, a 81-experiment design for 40 three-level factors [$N = 81$ and the factor values (1, 2, 3) are mapped onto $(0, +v, -v)$]. Although only 36 factors are required here, all of the array rows were used to maintain the balanced properties of the arrays.

B. Noisy Phenotype Methods

1. *Tsutusi and Ghosh's Method*

Tsutsui and Ghosh reported a noisy phenotype (NP) method for use with GA optimization.[4] During evaluation, a noise vector $\Delta\boldsymbol{n}$, uniformly distributed over the range $\pm v$, is added to $\boldsymbol{x}_j$. The fitness function is

$$\boldsymbol{f}_{\text{NP}}(\boldsymbol{x}_j) = f(\boldsymbol{x}_j + \Delta\boldsymbol{n}) \tag{3}$$

For this method $N = 1$, that is, no additional evaluations are required. The addition of noise to an unrobust design solution will alter its evaluated value. If the evaluation is worse, then it will immediately have a lower fitness. If the evaluation is improved, its higher fitness is unlikely to be sustained in subsequent generations as different values of noise are added. In comparison, a robust solution is one that is unaffected by $\Delta\boldsymbol{n}$. This method will produce both good and robust solutions and is distinct from those that simply add noise to the final evaluated value.[4] Some caveats in this method have been shown by Weismann et al.,[5] but because of the smoothness of the search space for this application these were not thought to be cause for concern.[6]

2. *Modified Tsutusi and Ghosh Method (NP2)*

The current authors modified the NP method so that both the true performance and the noisy performance were evaluated, the fitness

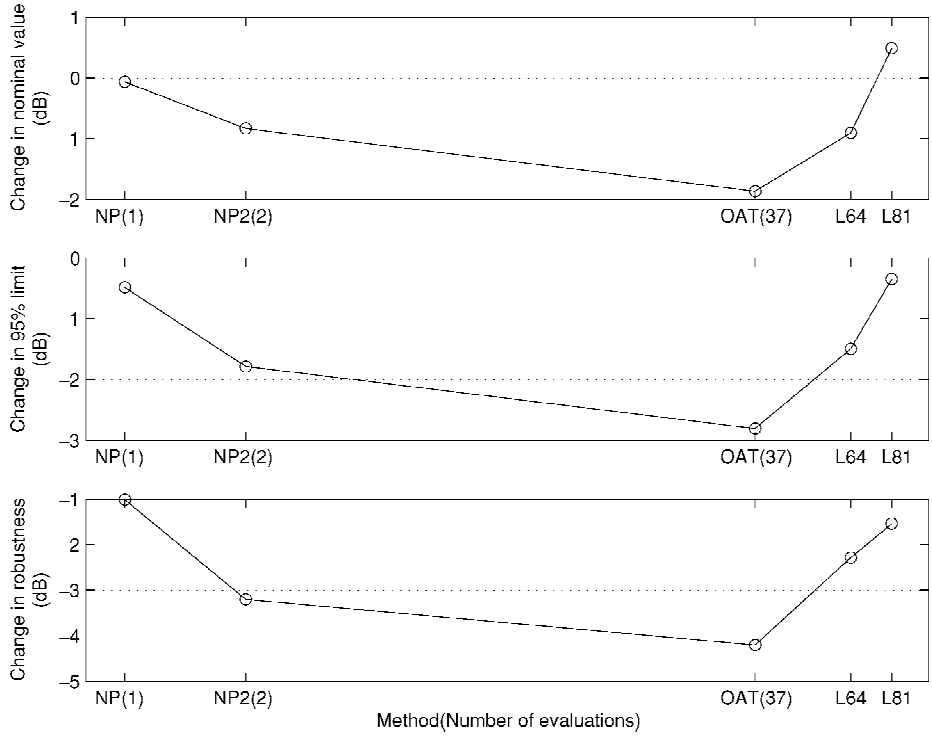

Fig. 2 Average change in nominal performance, 95% probability limit, and the robustness for the optimized structures achieved using the GAs detailed in the text, against structures produced using a nominal-performance objective function. (A negative change indicates improvement.)

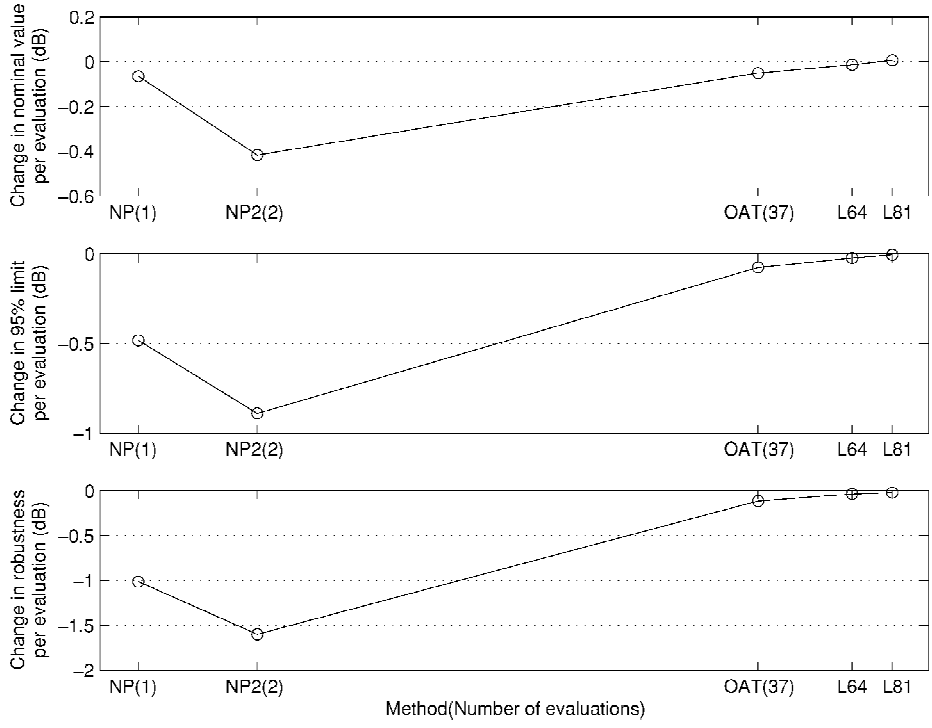

Fig. 3 Average change in nominal performance, 95% probability limit, and the robustness against structures produced using a nominal-performance objective function when normalized against the additional computational expense required.

function value being the worst of these two measures:

$$f_{\mathrm{NP2}}(\boldsymbol{x}_j) = \max[f(\boldsymbol{x}_j),\, f(\boldsymbol{x}_j + \Delta\boldsymbol{n})] \tag{4}$$

Thus, for this method $N = 2$. Functionally, this is only different from the NP method when an unrobust solution is evaluated with artificially high noise-induced performance. This will limit the short-term good fitness of these solutions. This modification might help increase the speed of convergence of the GA.

IV. Robust Optimization

Using the five different fitness functions, $\hat{f}_{95:\mathrm{OAT}}$, $\hat{f}_{95:\mathrm{L64}}$, $\hat{f}_{95:\mathrm{L81}}$, f_{NP}, and f_{NP2}, 10 structures were produced in each case using a different initial random number seed. The GA parameters were the same as those used to produce the structure shown in Fig. 1: five generations, each of population size 200, $p_{\mathrm{crossover}} = 0.8$, $p_{\mathrm{mutation}} = 0.005$, and an elitist strategy was used. Full details are given in Ref. 2. The v in each case was 0.005 m. The perturbation

vectors are only added during evaluation and do not permanently affect the design vectors $\boldsymbol{x}_j$ in the current GA population. The time to produce each structure is proportional to N. For the L81 method each structure took about 5.5 days to produce (compare, 1.7 h for the NP method, where $N = 1$) on an SGI hardware platform running at 90 MHz. After each optimization $f_{95:300}$ for the best resulting design from each GA, denoted by $\boldsymbol{x}_{\text{opt}}$, was evaluated to measure accurately the expected perturbed performance. The results are shown in Fig. 2, where the changes in the average values of $f(\boldsymbol{x}_{\text{opt}})$, $f_{95}(\boldsymbol{x}_{\text{opt}})$, and the robustness r for each method are compared with the average performance of the 10 structures previously optimized using a nominal performance-only measure. r is a measure of the variability of the performance defined as

$$r(\boldsymbol{x}_{\text{opt}}) = |f_{95}(\boldsymbol{x}_{\text{opt}}) - f(\boldsymbol{x}_{\text{opt}})| \tag{5}$$

Depending on the specific aim of the optimization, either the worst level of f_{95} or r might be of primary concern.

The robust-optimal structures are not shown for brevity, but it is noted that all of the structures have irregular and different geometries of the nature shown in Fig. 1, and there is no apparent characteristic to identify the optimal from the robust-optimal structures.[2]

V. Results and Discussion

Optimizing for both robust and optimal structures has not compromised the average nominal performance but further improved it by up to 2 dB, except for the L81 method where there was a small degradation. On average, all methods improved f_{95} and the robustness by up to 3 and 4 dB, respectively. Although the GA using $\hat{f}_{95:\text{OAT}}$ to estimate f_{95} had the best optimization performance, it has been shown that $\hat{f}_{95:\text{L64}}$ is the better estimator of f_{95} (Ref. 6). It is tentatively suggested that simply the use of geometric perturbations for GA optimization is more important for robust design than the precise details of the perturbations, especially as factor interactions were not considered.

In Fig. 3 the averaged results are normalized for the additional computational overhead for each method. It is seen that the success of the OAT method is achieved at the cost of a large increase in computational effort, whereas the NP2 method appears to provide improvements for little additional overhead. As the NP and NP2 methods require either no or double the computational effort, the consideration of robustness need not be expensive. It is, again tentatively, suggested that the NP and NP2 method are promising for efficient robust-optimal design using GAs of high-dimensional problems. There was no notable difference in the convergence speed between these two GAs.

Finally, it is noted that the damping ratio in the structure model (about 0.05 at 200 Hz) is higher than typically found in practice. Ongoing work on a practical three-dimensional structure suggests that this value could be 50 times too high.[7] With less damping more sensitivity to geometric perturbations is expected, and a higher reward would be gained from considering robustness in the optimization.

VI. Conclusions

The work briefly presented here has demonstrated various schemes that can be incorporated into a genetic algorithm (GA) to help ensure that robust designs result from such search processes. They are all based on incorporating minor perturbations to the configurations evolved by the GA to assess their robustness. Of the methods considered, a series of one-at-a-time variations to the parameters being optimized yields the most robust designs but at high computational cost. A modified noisy phenotype method is shown to be almost as effective at ensuring robustness while being much more computationally efficient.

References

[1]Mitchell, M., *An Introduction to Genetic Algorithms*, MIT Press, Cambridge, MA, 1996.

[2]Anthony, D. K., Elliott, S. J., and Keane, A. J., "Robustness of Optimal Design Solutions to Reduce Vibration Transmission in a Lightweight 2-D Structure. Part I: Geometric Redesign," *Journal of Sound and Vibration*, Vol. 229, No. 3, 2000, pp. 505–528.

[3]Taguchi, G., *System of Experimental Design*, UNIPUB/Kraus International Publications, New York, 1987.

[4]Tsutsui, S., and Ghosh, A., "Genetic Algorithms with a Robust Solution Searching Scheme," *IEEE Transactions on Evolutionary Computation*, Vol. 1, No. 3, 1997, pp. 201–208.

[5]Weismann, D., Hammel, U., and Bäck, T., "Robust Design of Multilayer Optical Coatings by Means of Evolutionary Algorithms," *IEEE Transactions on Evolutionary Computation*, Vol. 2, No. 4, 1998, pp. 162–167.

[6]Anthony, D. K., "Robust Optimal Design Using Passive and Active Methods of Vibration Control," Ph.D. Dissertation, Inst. of Sound and Vibration Research, Southampton Univ., Southampton, England, U.K., June 2000.

[7]Moshrefi-Torbati, M., Keane, A. J., Elliott, S. J., Brennan, M. J., and Rogers, E., "The Integration of Advanced Active and Passive Structural Vibration Control," *Proceedings of VETOMAC-I*, Indian Inst. of Science, Bangalore, India [CD-ROM)], edited by K. Venkatraman and C. S. Manohar, 2000.

A. Messac
Associate Editor

Illustration of the Inclusion of Sound–Flow Interactions in Lighthill's Equation

Christophe Bogey,* Xavier Gloerfelt,† and Christophe Bailly‡
Ecole Centrale de Lyon, 69134 Ecully, France

Introduction

LIGHTHILL'S equation[1] is an exact reformulation of the flow equations

$$\left(\frac{\partial^2}{\partial t^2} - c_0^2\nabla^2\right)\rho' = \frac{\partial^2 T_{ij}}{\partial x_i \partial x_j}(\boldsymbol{x}, t) \tag{1}$$

where $\rho' = \rho - \rho_0$ is the density fluctuation, ρ_0 and c_0 the ambient density and sound speed, and $T_{ij} = \rho u_i u_j + (p - c_0^2\rho)\delta_{ij} - \tau_{ij}$ the Lighthill stress tensor, with u_i the velocity components, p the pressure, and τ_{ij} the viscous stresses. The classical interpretation of Eq. (1) consists of regarding the aerodynamic noise as solution of a wave equation in a fictitious medium at rest. The sound generation is assigned to the right-hand side, through the tensor T_{ij}, which is reduced to $T_{ij} = \rho u_i u_j$ in unheated flows at high Reynolds numbers. Thus, as long as T_{ij} is known, evaluated from the unsteady Reynolds averaged Navier–Stokes equations,[2] from large eddy simulation,[3] or from direct numerical simulation,[4,5] Eq. (1) can be solved for noise predictions.

Because Lighthill's equation is based on a wave equation in a medium at rest, the right-hand side contains both sound generation and flow effects on propagation. Two parts can actually be identified

Received 23 April 2002; revision received 4 September 2002; accepted for publication 16 September 2002.

*Research Scientist, Laboratoire de Mécanique des Fluides et d'Acoustique, Unité Mixte de Recherche 5509 du Centre National de la Recherche Scientifique; christophe.bogey@ec-lyon.fr.

†Postdoctoral Student, Laboratoire de Mécanique des Fluides et d'Acoustique, Unité Mixte de Recherche 5509 du Centre National de la Recherche Scientifique.

‡Assistant Professor, Laboratoire de Mécanique des Fluides et d'Acoustique, Unité Mixte de Recherche 5509 du Centre National de la Recherche Scientifique. Member AIAA.